Creation of sine-Gordon solitons by a pulse force

Yuri S. Kivshar
Institute for Low Temperature Physics and Engineering, 47 Lenin Avenue, 310164 Kharkov, U.S.S.R.

Boris A. Malomed
P. P. Shirshov Institute of Oceanology, 23 Krasikov Street, 117234 Moscow, U.S.S.R.

Zhang Fei and Luis Vázquez
Departamento de Física Teórica, Facultad de Ciencias Físicas, Universidad Complutense, E-28040 Madrid, Spain

(Received 22 May 1990)

We study the problem of soliton generation by an external pulse force in the framework of the sine-Gordon system. The problem is applied to the creation of fluxons in long Josephson junctions or magnetic solitons in one-dimensional magnetic systems with an easy-plane anisotropy. In case of a small duration of driving pulse T, we find the connection between parameters of the pulse force and the wave field created after the pulse. To define the parameters of the generated soliton we use an approach based on the inverse scattering transform. The analytical results are presented in two cases when the spatial length L of the pulse is either much larger or much smaller than the value $V_g T$, V_g being the maximum value of the group velocity in the system. The threshold conditions admitting generation of either breathers or kink-antikink pairs are found. Numerical simulations are performed for arbitrary values of the ratio $L/V_g T$ but for small T. In two limiting cases the results are in good comparison with the obtained analytical formulas. The influence of dissipative losses on the soliton creation is also studied by analytical and numerical methods. It is demonstrated that dissipation leads to an increasing of the threshold conditions to generate solitons by the pulse force.

I. INTRODUCTION

The concept of the soliton plays an important role in modern solid-state physics. Well-known examples are long Josephson junctions (LJJ's) and magnetic systems including ferromagnets and antiferromagnets. Theoretical models of both these systems reduce to the sine-Gordon (SG) equation.[1,2] As is well known, this equation admits solitons of two distinct types: topological solitons (kinks) and nontopological ones (breathers). In the theory of LJJ's, a kink represents a fluxon, i.e., magnetic flux quantum.[1] In the theory of one-dimensional magnetic systems, a kink corresponds to a domain wall.[2]

An important physical problem is the generation of solitonic excitations in these systems. In LJJ's of the inline type, fluxons are created by application of a bias current pulse to an edge of the junction.[3,4] In LJJ's of the overlap type, they are created by application of the magnetic-field pulse.[5]

A spatially localized pulse of the magnetic field can also be employed to generate pairs of domain walls (DW's) and/or magnetic solitons (MS's) (breathers) in easy-plane ferromagnets.[6,7] Unlike DW's, MS's are sufficiently dynamical excitations, and the problems of their nonthermal creation and stabilization are very important from the viewpoint of recent experimental attempts to create and study the properties of the dynamical solitons in a few magnetic systems.[8-10]

The problem of soliton generation arises in any physical system admitting existence of solitonic excitations, and it is not easy to solve. The exact analytical results may be obtained only for the Cauchy problem when the equation of motion can be solved by the inverse scattering transform (IST). The IST method allows us to predict asymptotic evolution of an initial wave-field distribution defined at $t=0$, and, in particular, to calculate parameters of created solitary waves. In this connection it should be noted that a detailed analysis of some of the simplest initial SG wave-field configurations was carried out from the viewpoint of the IST in Refs. 11 and 12.

Experimental conditions are associated with another situation, when an intense and generally localized pulse force drives a system from equilibrium, and the external pulse force results in a wave-field distribution from which solitons may be created. This clearly indicates that the parameters of the excited solitons are, in the final analysis, determined by the characteristics of the pulse force, i.e., its intensity and duration.

The way to solve such a problem was briefly described by Kivshar and Malomed,[13,14] and the method is based on the IST. In view of the fact that the formulation of the soliton generation problem most adequately corresponds to an experimental situation, we briefly outline the general solution scheme. The problem of the linear response of a system to an external pulse acting during the time $0<t<T$ is examined at the first stage, assuming that the system was in equilibrium [$\phi=\phi_t=0$, where $\phi(x,t)$ is the wave field] prior to the action of the external pulse force ($t<0$), and the spatial wave-field distribution at time $t=T$ is also calculated. It is obvious that such a

calculation will be valid only if the force acts for a time T short enough so that the excited pulse cannot "creep away" due to dispersion. It is important that the analysis of the response to the external action can be carried out in the linear approximation.[13,14] Then, using the derived field configuration as the initial condition for the Cauchy problem for $t > T$, we can solve the direct scattering problem within the framework of IST (the second stage). This makes it possible to obtain a set of so-called scattering data of the discrete and continuous spectra, which describes the further evolution of the pulses. Specifically, if we know the discrete spectrum, it is possible to determine completely the parameters of excited solitons. Since the IST is strictly valid for exactly integrable systems only, the auxiliary factors (responsible for the break of the exact integrability conditions) can be investigated in the framework of perturbation theory for solitons[15] taking the solution of the Cauchy problem as a zeroth-order approximation. This represents the third stage in solving the soliton generation problem.

The above-mentioned papers[3,4] dealt with two limiting cases in the soliton generation problem when the spatial length of the pulse L is either larger or smaller than the value $V_g T$, V_g being the maximum value of the group velocity in the system. In both cases the results may be obtained using some approximations. This paper aims to consider the soliton generation problem in a general form for arbitrary values of the ratio $L/V_g T$ using analytical and numerical approaches. Our idea is to compare analytical results and numerical simulations and predict the dynamics of the system in more general cases when it cannot be solved analytically. This treatment and the obtained results have, in our view, a much broader applicability than to nonlinear wave generation in LJJ's and magnetic systems described by the SG equation. Indeed, any physical system that allows nonlinear soliton excitations to exist must deal with the problem of their generation. The situation where an intense and localized pulse drives a nonlinear system from equilibrium corresponds to experimental conditions. The force generates a wave-field distribution that can be considered as the initial data at $t = T$. If the system is described (after the end of external pulse action) by an exactly integrable equation, such as the SG equation, IST makes it possible, in principle, to calculate exactly the spectrum of the resulting excitations based on the wave-field configuration established by the pulse action. This approach may be applied to a number of other nonlinear systems.

The paper is organized as follows. In Sec. II we present the physical models that correspond to the soliton creation in LJJ's and an easy-plane ferromagnet (EPF). Section III is devoted to analytical analysis. Section IV describes the numerical simulations of the model and provides a comparison with the analytical formulas. Finally, the conclusions are presented in Sec. V.

II. PHYSICAL MODELS

A. Long Josephson junctions

A significant number of experimental and theoretical studies[1,3,4-5] have been devoted to investigation of the dynamics of Josephson vortices (magnetic flux quanta or fluxons) in LJJ's. Several methods can be used experimentally to excite fluxons in a long junction. One such method involves injecting an external current through the junction's edge; as a rule the injection current contains dc and pulsed components.[3] The resulting excitation of Josephson fluxons exhibits a threshold. The pulse area must exceed a certain critical value in order to generate a fluxon. This dynamical process was investigated numerically by Sakai and Samuelsen[4] in the framework of the semi-infinite LJJ model based on the SG equation (with a dissipative term) for the dimensionless magnetic flux $u(x,t)$,

$$u_{tt} - u_{xx} + \sin u + \gamma u_t = 0, \quad x > 0 , \tag{1}$$

which is supplemented by the boundary condition

$$u_x(0,t) = -h(t) . \tag{2}$$

The coordinate x, directed along the junction, and time t are measured in units of the Josephson penetration depth λ_J and the inverse Josephson frequency ω_J. The parameter γ phenomenologically accounts for dissipative losses stipulated by tunneling of normal quasiparticles through the junction; the term $-h(t)$ is the external bias current injected through the junctions' edge ($x = 0$). The same model describes the action of external variable magnetic field on the junction.

The current (or magnetic field) $h(t)$ may be represented as the sum of two terms,

$$h(t) = h_0 + h_1(t) , \tag{3}$$

where h_0 is the dc component of the current, while h_1 is the pulsed component.[3,4] Sakai and Samuelsen carried out numerical and semianalytical investigations of the pulsed component with a triangular wave form. We will provide a consistent analytical solution of the problem assuming a short duration T of the pulse injection current $h_1(t)$ as well as a dc current h_0. In the considered case the amplitudes of the pulsed injection current may reach substantial levels of the order of T^{-1}.

Bearing in mind the use of IST, we will continue Eq. (1) into the semiaxis $x < 0$ by the relation

$$u(-x,t) = u(x,t) . \tag{4}$$

Then the following equation will correspond to Eq. (1) with the boundary condition (2):

$$u_{tt} - u_{xx} + \sin u + \gamma u_t = 2h(t)\delta(x) . \tag{5}$$

Taking the parameter h_0 in (3) to be small, we will first consider the case $h_0 = 0$.

B. Easy-plane ferromagnets

Let us consider a ferromagnet with an easy-plane anisotropy (EPFM) in the presence of the external constant magnetic-field H lying in the basic plane. In an equilibrium state, the magnetization vector is directed along the field H. The deviation of the magnetization vector in the easy-plane from the field direction is characterized by the angle u, and its one-dimensional dynamics may be de-

scribed by the SG equation,[2,7,16]

$$u_{tt}-u_{xx}+\sin u=0 \ . \tag{6}$$

The coordinate x and the time t are measured in units of $(\alpha/H)^{1/2}$ and $\omega_0^{-1}=(\gamma M_0\sqrt{|\beta|H})^{-1}$, respectively. Here α and β ($\beta<0, |\beta|\gg 1$) are the exchange and anisotropy constants, and M_0 is the maximum magnetization. Small-amplitude deviations of u from the state $u\equiv 0$ are spin waves with the dispersion law $\omega^2=1+k^2$ and the group velocity

$$V_g=\frac{\partial\omega}{\partial k}=\frac{k}{(1+k^2)^{1/2}} \ . \tag{7}$$

To generate nonlinear excitations, one needs to apply an additional (pulsed) magnetic field $h(x,t)$ localized in the x direction. The direction of the field may be characterized by the angle χ between the fields H and $h(x,t)$. Then, according to Refs. 2 and 7, the equation of motion (6) takes the form

$$u_{tt}-u_{xx}+\left[1+\frac{h(x,t)}{H}\cos\chi\right]\sin u=\frac{h(x,t)}{H}\sin\chi \ . \tag{8}$$

As we can see from further analysis, the term $[h(x,t)/H]\cos\chi$ may be neglected, provided that either $\tan\chi\gg T/L$ in case $L\gg T$, or $\tan\chi\gg 1$ in case $L\ll T$.

C. Formulation of the problem

To consider both soliton generation problems (5) and (8) in a general form, we study the equation

$$u_{tt}-u_{xx}+\sin u+\gamma u_t=f(x,t) \ , \tag{9}$$

where

$$f(x,t)=\begin{cases} A, & |x|<L/2, \quad 0<t<T \\ 0, & |x|>L/2, \quad 0<t<T \\ 0, & t>T \ . \end{cases} \tag{10a}$$

In case of EPFM, the parameter A takes the form $A=(h_m/H)\sin\chi$, h_m being the amplitude of the pulsed magnetic field. For LJJ's we have to consider the limit $L\to 0$, with $AL<\infty$, so that $f(x,t)$ tends to a δ-like force,

$$f(x,t)=f(t)\delta(x) \ , \tag{11}$$

where

$$f(t)=2h(t)=\begin{cases} AL\equiv C, & 0<t<T \quad (12a) \\ 0, & t>T \ . \quad (12b) \end{cases}$$

C has the sense of the field at the junction's edge.

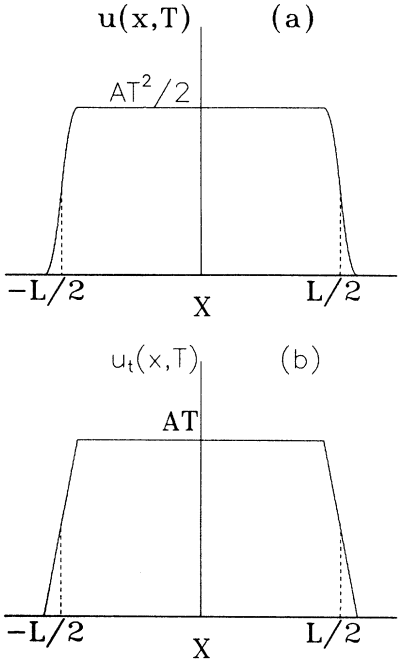

FIG. 1. (a) Function $u(x,T)$ defined by Eq. (14). (b) Function $u_t(x,T)$ defined by Eq. (15).

III. ANALYTICAL APPROACH TO THE SOLITON CREATION PROBLEM

A. Initial pulse wave form and solution of the direct scattering problem

1. *"Wide" pulse*

If the duration T of the pulse is small ($T\ll 1$), the results may be obtained analytically. In this case, for $t\le T$ the terms ϕ_{tt} and ϕ_{xx} are large, the wave field $\phi(x,t)$ changes sufficiently only at the points $x=\pm L/2$ in a vicinity $\Delta x\sim T\ll 1$, and the term $\sin u$ in (9) remains of order unity over the time T during which the pulsed force (10) acts. Consequently, during the action of the force, Eq. (9) can be replaced by the linear equation

$$u_{tt}-u_{xx}+\gamma u_t=f(x,t) \ . \tag{13}$$

The linear equation (13) can be solved exactly at the initial conditions $u(x,0)=u_t(x,0)=0$ and the pulsed force (10). Subsequent calculations by means of IST may be carried out only in two limiting cases, a "wide" pulse $L\gg T$, and a "narrow" pulse $L\ll T$, (or $L\to 0$ in case of LJJ's). First of all, we will consider the case of $\gamma=0$. The solution of Eq. (13) with the force (10) when $\gamma=0$ and at the moment $t=T$ has the form [see also Figs. 1(a) and 1(b)]

$$\begin{aligned} u(x,T)=-(A/8)\{&2(L/2+x)^2\mathrm{sgn}(L/2+x)+2(L/2-x)^2\mathrm{sgn}(L/2-x) \\ &-(L/2+x+T)^2\mathrm{sgn}(L/2+x+T)-(L/2+x-T)^2\mathrm{sgn}(L/2+x-T) \\ &-(L/2-x+T)^2\mathrm{sgn}(L/2-x+T)-(L/2-x-T)^2\mathrm{sgn}(L/2-x-T)\} \ , \end{aligned} \tag{14}$$

$$u_t(x,T)=(A/4)\{|L/2+x+T|-|L/2+x-T)|+|L/2-x+T|-|L/2-x-T|\} \ , \tag{15}$$

where

$$\mathrm{sgn}(x)\equiv\begin{cases}+1, & x>0\\ 0, & x=0\\ -1, & x<0\end{cases}.$$

To calculate the soliton parameters for $t>T$, we must employ the inverse scattering method where the functions $u(x,t)$ and $u_t(x,t)$ defined by Eqs. (14) and (15) are the initial "potentials." The IST allows us to solve the Cauchy problem.[17] In the inverse scattering technique, the SG equation is related to the linear scattering problem

$$\hat{L}(u,u_t;\lambda)\Psi(x,t;\lambda)=0 \tag{16}$$

for the auxiliary two-component Jost function

$$\Psi(x,t;\lambda)=\begin{bmatrix}\Psi_1(x,t;\lambda)\\ \Psi_2(x,t;\lambda)\end{bmatrix},$$

where λ is the spectral parameter, which takes real positive values. The operator $\hat{L}$ has the form

$$\hat{L}=\hat{I}\frac{\partial}{\partial x}-\frac{i}{2}\left[\left[\lambda-\frac{1}{4\lambda}\cos u\right]\hat{\sigma}_3-\frac{\hat{\sigma}_2}{4\lambda}\sin u+\frac{\hat{\sigma}_1}{2}(u_x-u_t)\right], \tag{17}$$

where $\hat{\sigma}_\alpha$ $(\alpha=1,2,3)$ are the Pauli matrices, and $\hat{I}$ is the unit matrix.

The so-called amplitudes (Jost coefficients) play an important role in the inverse scattering technique. To define the amplitudes, let us consider the eigenfunction $\Psi(x,\xi;\lambda)$ with the asymptotic at $x\to-\infty$,

$$\Psi(x;\lambda)\to\Psi_-(x,\xi;\lambda)\equiv\begin{bmatrix}0\\ e^{-(i/2)k(\lambda)x}\end{bmatrix}, \tag{18}$$

where

$$k(\lambda)\equiv\lambda-\frac{1}{4\lambda}. \tag{19}$$

At $x\to+\infty$ the function may be presented as follows:

$$\Psi(x;\lambda)\to\Psi_+(x;\xi;\lambda)\equiv\begin{bmatrix}b(\lambda)e^{(i/2)k(\lambda)x}\\ a(\lambda)e^{-(i/2)k(\lambda)x}\end{bmatrix}. \tag{20}$$

The functions $b(\lambda$ and $a(\lambda)$ are the Jost coefficients, and they describe properties of the solutions at $t>0$.

According to IST, soliton excitations of the nonlinear system correspond to solutions of the equation $a(\lambda_n)=0$ with $\mathrm{Im}\lambda_n>0$ [zeros of $a(\lambda)$ lying in the upper half-plane of λ]. If the initial pulse $u(x,t)$ is an even function in x, the solutions λ_n may appear only by pairs (see details in Refs. 11–14). The conjugate pair of the solutions, $\lambda_{1,2}=\pm\frac{1}{2}\exp(\pm i\mu)$, corresponds to a quiescent breather with an amplitude $0<\mu<\pi/2$ and the frequency $\cos\mu$:

$$u_{\mathrm{br}}=4\tan^{-1}\left[\tan\mu\frac{\sin(t\cos\mu+\phi_0)}{\cosh(x\sin\mu)}\right], \tag{21}$$

ϕ_0 being a constant initial phase. The pair of purely imaginary zeros, $\lambda_{1,2}=\frac{1}{2}i\sqrt{(1\pm v)/(1\mp v)}$, corresponds to a kink-antikink solution that describes a scattering of a kink and antikink with opposite velocities $\pm v$. The SG kink is related to one zero $\lambda_1=\frac{1}{2}i\sqrt{(1+v)/(1-v)}$ and has the form

$$u_k(x,t)=4\sigma\tan^{-1}\exp\left[-\frac{x-\xi}{(1-v^2)^{1/2}}\right], \tag{22}$$

where σ is the kink polarity ($\sigma=+1$ corresponds to a kink and $\sigma=-1$ to an antikink), and $\xi=vt+x_0$ is its coordinate.

Therefore, to find which type of initial function generates solitons and to determine their parameters, we have to investigate the direct scattering problem (16) with the initial functions (14) and (15). When the conditions

$$T\ll 1 \quad\text{and}\quad ATL\sim 1 \tag{23}$$

hold, the direct scattering problem (16) and (17) can be solved using the perturbation theory, provided $L\gg T$. Indeed, taking into account (23), we may estimate our functions as follows:

$$u_t\sim 1,\quad u\sim T\ll 1,\quad u_x\sim u/L\sim T/L\ll 1. \tag{24}$$

The estimations mean that, for $L\gg T$, we may use the following initial conditions as a "zeroth-order approximation:"

$$u^{(0)}(x,T)=0, u_t^{(0)}(x,t)=\begin{cases}AT\equiv B, & |x|<L/2\\ 0, & |x|>L/2,\end{cases} \tag{25}$$

and a departure of (14) and (15) from (25) may be taken into account as a perturbation. The approach is very fruitful because the direct scattering problem with the initial pulse (25) has been solved analytically.[11,12] According to Ref. 11, the initial conditions (25) lead to the following Jost coefficients:

$$a^{(0)}(\lambda)=e^{ik(\lambda)L/2}\left[\cos(\kappa L)-\frac{ik(\lambda)}{2\kappa}\sin(\kappa L)\right], \tag{26}$$

$$b^{(0)}(\lambda)=-\frac{iAT}{4\kappa}\sin(\kappa L), \tag{27}$$

where $\kappa^2\equiv\frac{1}{4}k^2(\lambda)+\frac{1}{16}B^2$. The additional term to $a^{(0)}(\lambda)$ may be calculated according to the formula of the perturbation theory,

$$a^{(1)}=\int_{-\infty}^{+\infty}dx\left[\left[\frac{\delta a}{\delta u}\right]_0\delta u+\left[\frac{\delta a}{\delta u_t}\right]_0\delta u_t\right], \tag{28}$$

where

$$\delta u\equiv u(x,T)-u^{(0)}(x,T),$$

$$\delta u\equiv u_t(x,T)-u_t^{(0)}(x,T),$$

and the variational derivatives,

$$\frac{\delta a}{\delta u_t(x)}=-\frac{i}{4}[\Psi_1(x,\xi;\lambda)\Phi_1(x,\xi;\lambda)-\Psi_2(x,\xi;\lambda)\Phi_2(x,\xi;\lambda)], \tag{29}$$

$$\frac{\delta a}{\delta u(x)} = + \frac{k(\lambda)}{4}[\Psi_1(x,\xi;\lambda)\Phi_1(x,\xi;\lambda) + \Psi_2(x,\xi;\lambda)\Phi_2(x,\xi;\lambda)] , \quad (30)$$

must be calculated in the zeroth approximation corresponding to (25). In (29) and (30), the functions $\Phi_{1,2}$ are the components of the second Jost function defined by its asymptotic at $x \to +\infty$,

$$\Phi(x,\lambda) \to \Phi_-(x,\lambda) \equiv \begin{bmatrix} e^{ik(\lambda)x/2} \\ 0 \end{bmatrix} \text{ as } x \to -\infty , \quad (31)$$

$$\Phi(x,\lambda) \to \Phi_+(x,\lambda) \equiv \begin{bmatrix} a(\lambda)e^{ik(\lambda)x/2} \\ b^* e^{-ik(\lambda)x/2} \end{bmatrix} \text{ as } x \to +\infty , \quad (32)$$

where the asterisk denotes complex conjugation. The Jost functions $\Psi(x,t)$ and $\Phi(x,t)$ corresponding to the initial conditions (25) were calculated in[11]

$$\Psi(x,\lambda) = \begin{cases} \Psi_-(x,\lambda) = \Psi_-(x,\lambda), & x < -L/2 , \quad (33) \\ \begin{bmatrix} -\frac{A}{B}(A_1\kappa_+ e^{i\kappa x} - A_2\kappa_- e^{-i\kappa x}) \\ A_1 e^{i\kappa x} + A_2 e^{-i\kappa x} \end{bmatrix}, & x < L/2 \quad (34) \\ \Psi_+(x,\lambda), & x > L/2 , \quad (35) \end{cases}$$

$$\Phi(x,\lambda) = \begin{cases} \Phi_-(x,\lambda), & x < -L/2 \quad (36) \\ \begin{bmatrix} A_2 e^{i\kappa x} + A_1 e^{-i\kappa x} \\ -\frac{4}{B}(A_2\kappa_- e^{i\kappa x} - A_1\kappa_+ e^{-i\kappa x}) \end{bmatrix}, & |x| < L/2 \quad (37) \\ \Phi_+(x,\lambda), & x > L/2 , \quad (38) \end{cases}$$

where

$$A_1 \equiv \frac{\kappa_-}{2\kappa} e^{i\kappa_+ L/2} , \quad A_2 \equiv \frac{\kappa_+}{2\kappa} e^{-i\kappa_- L/2} , \quad \kappa_\pm \equiv \kappa \pm \frac{k(\lambda)}{2} . \quad (39)$$

Substituting (33)–(39) into (28) we can calculate the total Jost coefficient,

$$a(\lambda) = a^0(\lambda) + a^1(\lambda) = e^{ik(\lambda)L/2}\left[\cos(\kappa L) - \frac{ik(\lambda)}{2\kappa}\left[1 + \frac{B^2T^2}{24}\right]\sin(\kappa L)\right] . \quad (40)$$

The result (40) allows us to analyze the parameter of the created solitons (breathers or kink-antikink pairs).

2. A "narrow" pulse

Let us consider another limit case, $L \ll T$. In this case the pulse force may take the form (11), i.e., as a point force.

The linear wave equation (13) defined on the entire x axis is easily solved, and at the moment T, when the pulse ends, configuration of the wave fields $u(x,t)$ and u_t takes the form

$$u(x,T) = \frac{C}{2}\left[-|x| + \tfrac{1}{2}|x+T|\left[1 + \frac{\gamma}{4}(x-T)\right] + \tfrac{1}{2}|x-T|\left[1 - \frac{\gamma}{4}(x+T)\right]\right] , \quad (41)$$

$$u_t(x,T) = \frac{C}{4}(1 - \tfrac{1}{2}\gamma T)[\mathrm{sgn}(x+T) - \mathrm{sgn}(x-T)] , \quad (42)$$

where $C \equiv AL$. The functions are represented in Figs. 2(a) and 2(b) for $\gamma = 0$ and $\gamma \neq 0$. In order to describe the later evolution of the pulse we will examine, as in the case $L \gg T$, the functions (41) and (42) as initial conditions for the direct scattering problem (16) and (17).

If the conditions (23) hold, the direct scattering problem for the initial conditions (41) and (42) can be solved approximately. To this end, we write Eqs. (16) and (17) as follows:

$$\frac{\partial}{\partial x}\Psi_1 = a(x,\lambda)\Psi_1 + \beta(x,\lambda)\Psi_2 , \quad (43)$$

$$\frac{\partial}{\partial x}\Psi_2 = -\alpha(x,\lambda)\Psi_2 - \beta^*(x,\lambda)\Psi_1 , \quad (44)$$

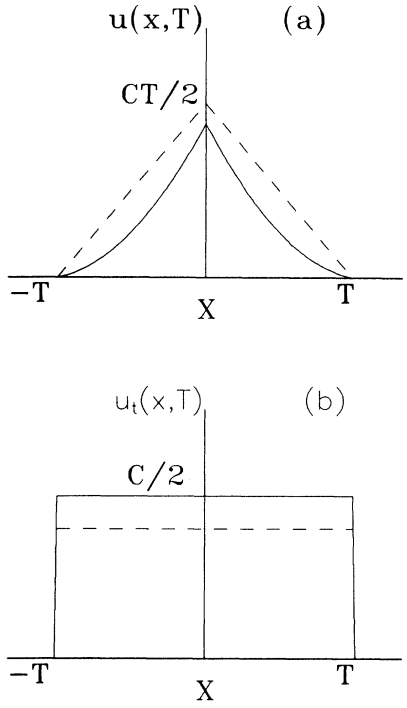

FIG. 2. (a) Function $u(x,T)$ defined by Eq. (41). The dashed line corresponds to $\gamma=0$ and the solid line to $\gamma\neq 0$. (b) Function $u_t(x,T)$ defined by Eq. (42). The solid line corresponds to $\gamma=0$ and the dashed line to $\gamma\neq 0$.

where

$$\alpha(x,\lambda)\equiv\frac{i}{2}\left[\lambda-\frac{1}{4\lambda}\cos u\right], \tag{45}$$

$$\beta(x,\lambda)\equiv\frac{i}{2}(u_x-u_t)-\frac{1}{8\lambda}(\sin u) \tag{46}$$

In order to find the scattering data, we will specify the asymptotic values of the function Ψ for $x\to\pm\infty$ as in Eqs. (18) and (20). After this normalization has been chosen, the solution of Eqs. (43) and (44) for $x<-T$ (see Fig. 2) obviously has the form (18).

As the subsequent analysis will demonstrate, it is sufficient to know the behavior of the amplitude $a(\lambda)$ for $k\sim 1$, i.e., near the point $\lambda=\pm\frac{1}{2}$, in order to investigate the soliton creation. For $k(\lambda)\ll T^{-1}$ the direct scattering problem can be solved approximately in each of the following intervals specified by the initial conditions (41) and (42).

a. The interval $-T<x<0$. Introducing the notation $y\equiv D(x+T)$, where $D\equiv C(x-\frac{1}{2}\gamma T)$, we will represent the initial conditions (41) and (42) as

$$u=y+\frac{\gamma}{4D}y(y-2DT),\quad u_x-u_t=\frac{\gamma y}{2}, \tag{47}$$

where $y\sim 1$. Taking into account that $D\sim T^{-1}\gg 1$ [see Eq. (23)], we will find the solution of Eqs. (43) and (44) as the first term of a series in powers of $D^{-1}\sim T$:

$$\Psi_1=\frac{i\gamma}{16D}Fy^2+\frac{F}{8\lambda B}(\cos y-1),$$

$$\Psi_2=F-\frac{iF}{2D}\left[\lambda y-\frac{1}{4\lambda}\sin y\right]. \tag{48}$$

The constant F is determined from the matching conditions at $x=-T$. $(y=0)$ for the function (48) with the function $\Psi_-(x,\lambda)$ defined in Eq. (18):

$$F=\exp\left[\frac{i}{2}k(\lambda)T\right]. \tag{49}$$

b. The interval $0<x<T$. We introduce the notation $z\equiv D(x-T)$ and represent the initial conditions (41) and (42) as

$$u=-z+\frac{\gamma z}{4D}(z+2DT),\quad u_x-u_t=2D-\frac{\gamma}{2}(z+2DT). \tag{50}$$

We note that by virtue of condition (23) $z\sim 1$, since $D\gg 1$ and $DT\sim 1$, as before, an approximate solution of Eqs. (43) and (44) at this interval takes the form

$$\Psi_1=[C_1+A_1(z)]e^{iz/2}+[C_2+A_2(z)]e^{-iz/2}, \tag{51}$$

$$\Psi_2=-[C_1+A_1(z)]e^{iz/2}+[C_2+A_2(z)]e^{-iz/2}, \tag{52}$$

where

$$A_1(z)=-\frac{C_2}{2D}\left[\lambda e^{-iz}+\frac{iz}{4\lambda}\right]-\frac{i\gamma C_1}{8D}\left[\frac{z^2}{2}+2DTz\right]+G_1, \tag{53}$$

$$A_2(z)=\frac{C_1}{2D}\left[\lambda e^{iz}-\frac{iz}{4\lambda}\right]+\frac{i\gamma C_2}{8D}\left[\frac{z^2}{2}+2DT_z\right]+G_2, \tag{54}$$

while the constants C_1, C_2, G_1, and G_2 must be determined from the matching conditions for the Jost functions in each order in the small parameter $D^{-1}\sim T$. At the lowest order we have

$$C_1=-\frac{F}{2}e^{iDT/2},\quad C_2=\frac{F}{2}e^{-iDT/2}. \tag{55}$$

In order to simplify the process of calculating final results we will express the Jost coefficient $a(\lambda)$ directly through the constants G_1 and G_2 determined in Eqs. (53). We find from matching the functions (51) and (52) to Ψ_+ at $x=T(z=0)$:

$$a(\lambda)e^{-ik(\lambda)T/2}=\Psi_2|_{x=0}=F\cos\left[\frac{DT}{2}\right]-\frac{i\lambda F}{2D}\sin\left[\frac{DT}{2}\right]+(G_2-G_1). \tag{56}$$

We have used Eq. (55) in writing (56). By matching the functions (51) and (52) to the functions (48) at $x=0$, it is

possible to find G_2-G_1 to the first order in D^{-1}, which finally yields

$$a(\lambda)\equiv a(k(\lambda))=e^{ikT}\left[(1-ikT/2)\cos\left[\frac{DT}{2}\right]+\frac{\gamma DT^2}{4}\sin\left[\frac{DT}{2}\right]-\frac{ik}{D}\sin\left[\frac{DT}{2}\right]\right]. \quad (57)$$

$k\equiv k(\lambda)$ is defined in (19). It is possible to find another Jost coefficient $b(\lambda)$ analogously:

$$b(\lambda)=-ie^{-ikT}\left[\left(1-\frac{ikT}{2}\right)\sin\left[\frac{DT}{2}\right]+\frac{i\gamma DT^2}{4}\cos\left[\frac{DT}{2}\right]\right]. \quad (58)$$

We point out that the results (57) and (58) are valid under conditions (23) and also for $k\ll T^{-1}$.

B. Analysis of the scattering data

According to the IST results, the zeros of the Jost coefficient $a(\lambda)$ correspond to solitons; these lie in the upper half plane of the complex spectral parameter λ (see Fig. 3). A breather, the kink-antikink bound state oscillating with the frequency $\cos\mu$ [see Eq. (21)], corresponds to the complex-conjugate pairs of the roots

$$\left.\begin{matrix}\lambda_1\\ \lambda_2\end{matrix}\right\}=\pm\exp(\pm i\mu) \quad (59)$$

and has the form (21). A pair of purely imaginary roots,

$$\left.\begin{matrix}\lambda_1\\ \lambda_2\end{matrix}\right\}=\tfrac{1}{2}i\sqrt{(1\mp v)/(1\pm v)}\,, \quad (60)$$

corresponds to the solution

$$u_{K\bar{K}}(x,t)=4\tan^{-1}\left\{\frac{\sinh[vt/(1-v^2)^{1/2}+\psi_0]}{v\cosh[x/(1-v^2)^{1/2}]}\right\}, \quad (61)$$

which describes a collision of a kink and an antikink with the velocities $\pm v$. The symmetry of the solution (61) and (21) is related to the condition $u(-x,t)=u(x,t)$. In the case of LJJ's, it is in fact obvious that only a kink traveling at a positive velocity [having the polarity $\sigma\equiv\mathrm{sgn}(A)$] is physically meaningful (its partner traveling with negative velocity is its "mirror image" with respect to the junction's edge $x=0$). Similarly, for $x>0$, the breather solution in fact describes a single kink (fluxon) oscillating in the effective potential well near the junction's edge. Substituting expressions (40) or (57) into the equation $a(\lambda)=0$, we can define parameters of the created solitons. Let us consider the parameters separately for both cases.

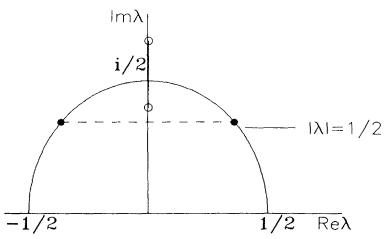

FIG. 3. The eigenvalues of the discrete spectrum λ. The solid circles correspond to a breather and the white ones to a kink-antikink pair.

1. The case $L\gg T$

Equations (40) and $a(\lambda)=0$ lead to the equation

$$\cot(\kappa L)=\frac{ik}{2\kappa}(1+B^2T^2/24)\,, \quad (62)$$

where $\kappa^2\equiv 1/4k^2+1/16B^2$, and $k\equiv k(\lambda)$ is defined in Eq. (19). The analysis of solutions lying in the upper half plane of λ is similar to that performed in Refs. 11 and 12. The results are the following: A breather will be generated in the system by the pulsed force if the pulse "volume" $BT\equiv ALT$ exceeds the threshold

$$(ALT)^{\mathrm{br}}_{\mathrm{thr}}=2\pi\,. \quad (63)$$

Similarly, from Eq. (62) we can obtain the threshold condition for generation of N breathers,

$$ALT\geq(ALT)^{N\,\mathrm{br}}_{\mathrm{thr}}=2\pi(2N-1)\,. \quad (64)$$

The search for the threshold conditions for the creation of free kinks, i.e., kink-antikink pairs (61), and determination of their initial velocities are of fundamental interest. The zeros λ will be purely imaginary when $k(\lambda)=ik_0$. In this case the velocities of the created kink and antikink may be presented as

$$v_{1,2}=\pm v=\pm\frac{(k_0^2-1)^{1/2}}{k_0}\,. \quad (65)$$

The parameter k_0 is defined by the equation

$$z\cot z=-[(LB/4)^2-z^2]^{1/2}(1+B^2T^2/24)\,, \quad (66)$$

where

$$z\equiv\tfrac{1}{2}L(B^2/4-k_0^2)^{1/2}\,. \quad (67)$$

At the threshold of the kink-antikink creation, the relations $v=0$ and $k_0=1$ hold. Analysis of solutions of Eq. (66) leads to the condition

$$ALT\geq(ALT)^{K\bar{K}}_{\mathrm{thr}}=F(L)\,, \quad (68)$$

where the function $F(L)$ is defined by the transcendental equation

$$(F^2-4L^2)^{1/2}\cot[(F^2-4L^2)^{1/2}/4]=-2L(1+B^2T^2/24)\,. \quad (69)$$

The function $F(L)$ is monotone increasing, at $L=0$ its value is $F(0)=2\pi$, and for $L\gg 1$ it has the asymptotic

$$F(L)\simeq 2L+4\pi^2/L\,. \quad (70)$$

In connection with Eqs. (69) and (70) it is necessary to note that the above results are obtained in the region

$$T \ll L \ll T^{-1} . \tag{71}$$

In this region the function $F(L)$ has the property $F(L) > 2L$. As we can see from Eq. (69), the corrections of the order of T^2 shift, in a general case, the threshold for a kink-antikink pair creation, but these do not affect the breather's threshold (63).

2. The case $L \ll T$

Substituting expression (57) into $a(\lambda)=0$ yields the equation

$$\left[1-\frac{ikT}{2}\right]\cot\frac{DT}{2}+\frac{\gamma DT^2}{4}=\frac{ik}{D} , \tag{72}$$

where $D \equiv C(1-\gamma T/2)= AL(1-\gamma T/2)$. Let $\gamma=0$ as in the above case; then a simple analysis shows that the breather is generated by the pulse if the "pulse area" exceeds the threshold ($D=C$ at $\gamma=0$),

$$(CT)_{\rm thr} \equiv (ALT)^{\rm br}_{\rm thr}=2\pi . \tag{73}$$

Similarly, from Eq. (72) we obtain the threshold condition for generation of N breathers, which is exactly the sane as Eq. (64).

The threshold condition corresponding to a kink-antikink pair creation takes the form $a(k=i)=0$, i.e., free kinks are generated when

$$ALT \geq (ALT)^{K\bar{K}}_{\rm thr}=2\pi+4T/\pi . \tag{74}$$

The threshold conditions for generation of N free pairs can be found analogously:

$$ALT \geq (ALT)^{NK\bar{K}}_{\rm thr}=2\pi(2N-1)+4T/\pi(2N-1) . \tag{75}$$

The polarities of all generated kinks (in the physical domain $x>0$) are equal to the sign of the amplitude A.

C. Radiative losses

In addition to the breathers and kink-antikink pairs, the applied pulse also generates nonsoliton excitations (linear wave packets) described by the continuous spectrum in terms of the IST method. The primary characteristic of the continuous spectrum is the scattering amplitude $b(\lambda)$ defined in Eqs. (27) or (58). Specifically, at the generation threshold for a kink-antikink pair, i.e., when the equality in relation (74) holds, we have for (58) ($k \ll T^{-1}$)

$$b(\lambda)=-i\cos(T/\pi) . \tag{76}$$

The fundamental physical characteristic of these waves is the spectral density $\varepsilon(k)=dE_{em}/dk$ of their energy E_{em}. According to IST (see Ref. 17),

$$\varepsilon(k)=\pi^{-1}\ln(1-|b(k)|^2)^{-1} . \tag{77}$$

Using relation (77), it is possible to estimate the energy contained in the nonsoliton part of the pulse-generated wave field at the threshold (63) as

$$E_{em} \equiv \int_0^\infty \varepsilon(k)dk$$

$$=\frac{4}{\pi L}\int_0^\infty dx \ln\left[1-\frac{\pi^2}{x^2+\pi^2}\sin^2[(x^2+\pi^2)/2]\right]^{-1}$$

$$\sim \frac{\text{const}}{L}, \quad L \gg T \tag{78}$$

and

$$E_{em}=\int_0^\infty \varepsilon(k)dk=\frac{1}{T}\int_0^1 \varepsilon(x/T)dx \sim \text{const}\frac{1}{T}, \quad L \ll T . \tag{79}$$

It is interesting to compare the values of (78) and (79) with the input energy generated by the pulsed force. Multiplying Eq. (9) at $\gamma=0$ and integrating by part, we obtain

$$\frac{dE}{dt}=\int_{-\infty}^{\infty} f(x,t)u_t dx , \tag{80}$$

where E is the total energy of the SG system,

$$E=\int_{-\infty}^{\infty} dx[\tfrac{1}{2}u_t^2+\tfrac{1}{2}u_x^2+(1-\cos u)] . \tag{81}$$

Considering $u(x,0)=0$, $u_t(x,0)=0$, and $E(t=0)=0$, we can obtain from Eq. (80) the total input energy:

$$\begin{aligned} E_{\rm input}=E(t=T)&=\int_0^T dt\int_{-\infty}^{\infty} f(x,t)u_t dx \\ &=A\int_0^T dt\int_{-\infty}^{\infty} dx\,[\theta(t)-\theta(t-T)][\theta(x+L/2)-\theta(x-L/2)]u_t(x,t) \\ &=A\int_{-L/2}^{L/2} u(x,T)dx . \end{aligned} \tag{82}$$

Using the results (14) and (41), we can represent (82) as follows:

$$E_{\rm input}=\begin{cases} \frac{1}{2}A^2LT^2, & \text{if } L \gg T \\ \frac{1}{2}A^2L^2T, & \text{if } L \ll T . \end{cases} \tag{83}$$

At the threshold of breather generation defined by the relation $(ALT)_{\rm thr}=2\pi$, we have the simple relations

$$E_{\rm input}=\begin{cases} 2\pi^2/L, & \text{if } L \gg T \\ 2\pi^2/T, & \text{if } L \ll T . \end{cases} \tag{84}$$

Comparing (84) to the energy E_{em} of the created radia-

tion, we find that the values are of the same order, and only a small fraction of the input energy is expended on the creation of the kink near the threshold (in our notation, the kink's energy is $E_k=8$). All the remaining energy is expended on creation of the relatively "useless" nonsoliton wave field. We note that the case $L \gg T$ is more effective because in this case we can obtain

$$E_{\text{input}}=\tfrac{1}{2}A^2LT^2 \sim \tfrac{1}{2}F^2(L)/L \sim E_k+E_k \sim 1 \ .$$

That is not possible in the other case because $T \ll 1$. As a result, the radiation part of the generated wave field is much greater than the soliton part in the case $L \ll T$.

D. Dissipative losses and stabilization of the created solitons

In the framework of the approach developed above, we can take into account dissipative losses during the action of the pulsed force. The calculations of the generated wave field at $\gamma \neq 0$ is similar to those presented, and, in fact, they have been done in the case $L \ll T$ [see Eqs. (41), (42), (57), (58), and (72)]. The dissipative losses lead to increasing of all thresholds of soliton creation. In particular, at $\gamma \neq 0$ the breather threshold for both of the cases has the form

$$ALT \geq 2\pi(1+\gamma T) \ . \tag{85}$$

It is clear from (85) that the presence of dissipation in the system requires an increase of the input power in order to generate the same number of fluxons. The evolution of an initial pulse in a dissipative SG system was studied numerically in Ref. 18, which also noted the same trend.

In analyzing the dynamics of the initial pulse for times $t > T$ we have so far neglected the influence of dissipation on the nature of the kink motion. In fact, oscillations of the breather will experience a slow damping due to dissipation, and this bound state vanishes at $t \to \infty$, i.e., the kink is annihilated with the antikink. They decay of the breather amplitude for $\mu \ll 1$ is described by the exponential law:[19,20] $\mu=\mu(0)\exp(-2\gamma t)$. To stabilize the breather oscillations, one needs to apply an additional ac field to the system. In the case of LJJ's the force is the ac magnetic fields, $h_1=h_m\cos(\omega t)$, applied to the junction's edge and acting after the pulse has ended, i.e, at $t > T$. In the case of EPFM, one can use the parametrical pumping directed along the magnetic field H, $H \to H+H_m\cos(\omega T)$, the frequency ω of the pumping must be near the double frequency ω_0. Taking into account the results of Ref. 21, which is devoted to the analytical study of the stabilization by the parametrical pumping, we can conclude that in the region

$$\gamma < H_m < [\gamma^2+(\omega_0-\omega/2)^2]^{1/2} \tag{86}$$

the breather is stabilized on the frequency $\omega/2$ and its amplitude is

$$\mu_*=\tfrac{1}{2}[(\omega_0-\omega/2)+(H_m^2-\gamma^2)^{1/2}]^{1/2} \ . \tag{87}$$

Regarding the free kinks generated by the pulse when the conditions (68) or (74) hold, the motion of the kink is decelerated by dissipation according to the equation $dv/dt=-\gamma v$ and by a certain time t_0 it ends up at a point located at a distance of $\xi_0=v/\gamma$. As a result, the distance between the kink and antikink will be $2\xi_0$ (here v_0 is the initial velocity of the kinks). If the weak attractive force F_{attr} of the partner in the pair is ignored, $t_0=\infty$. In fact, t_0 is finite, and under the action of F_{attr} the kink will eventually travel backward and enter a bound state with the antikink in the form of a breather, which will be damped because of the dissipation. The expression for the force F_{attr} for $\xi \gg 1$ (ξ is the effective kink's coordinate measured from the point $x=0$) is well known[22]:

$$F_{\text{attr}} \approx -e^{-2\xi} \ . \tag{88}$$

If, in addition to the dissipation, we take account of a small dc component h_0 of the applied current injected through the junctions edge (the case of LJJ's), the resulting kink may go to infinity because the field leads to an auxiliary force

$$F_{\text{rep}}=4\sigma h_0 e^{-\xi}, \quad \sigma h_0 > 0 \ . \tag{89}$$

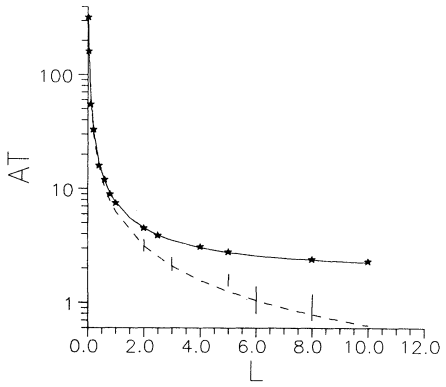

FIG. 4. The threshold for creating kink-antikink pair [solid line, defined by Eq. (69)], and that for creating breather [dashed line, defined by Eq. (63)]. Stars and bars are corresponding numerical results.

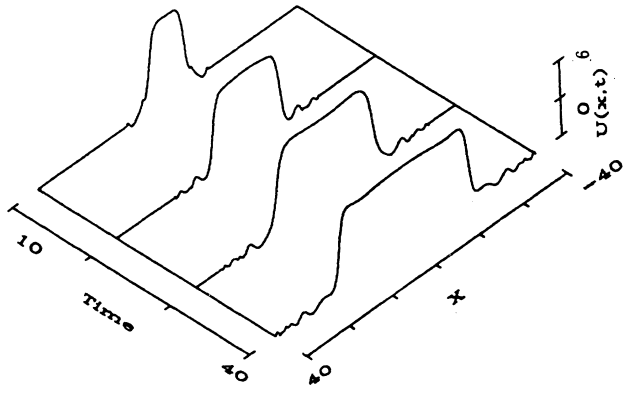

FIG. 5. Creation of kink-antikink pair, with parameters $T=0.1$, $L=5$, and $A=30$.

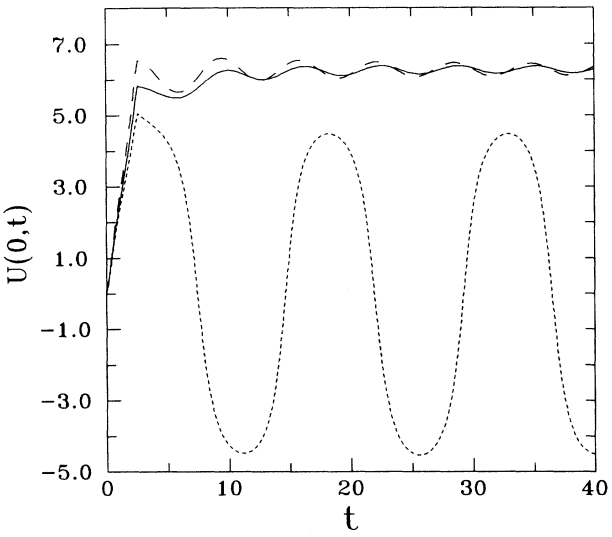

FIG. 6. $u(0,t)$ vs time for different A. The solid line is for $A=28$, the line is for dashed $A=30$, and the dotted line is for $A=26$. The pulse time is $T=0.1$ with length $L=5$.

As a result, we can conclude that when the dissipation is present a kink will escape from the bound state if its initial velocity v exceeds the critical value:

$$v_{\rm cr}=\gamma \ln|h_0|^{-1} . \tag{90}$$

The analogous result is valid in the case of EPFM in which the additional magnetic field $H_\perp$ directed perpendicular to the magnetic field H is applied; this time $h_0 \to H_\perp$ in Eq. (90).

The condition $V^2 > V_{\rm cr}^2$ suggests that in addition to the threshold values $A_1 = A_{\rm thr}^{\rm br}$, $A_2 = A_{\rm thr}^{K\bar{K}}$, . . . , at fixed L and T [see Eqs. (63), (68), (73), and (74)], there is a certain auxiliary threshold value $A_* > A_1$ for the kink going to infinity. If $\gamma \ln|h_0|^{-1} < 1$, then A_* lies in the range

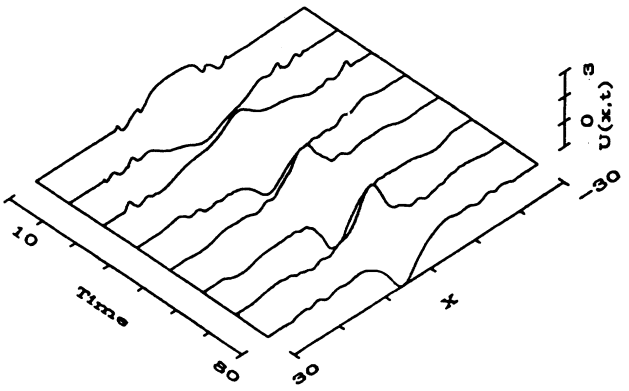

FIG. 7. Creation of breather, with parameters $T=0.1$, $L=5$, and $A=18$.

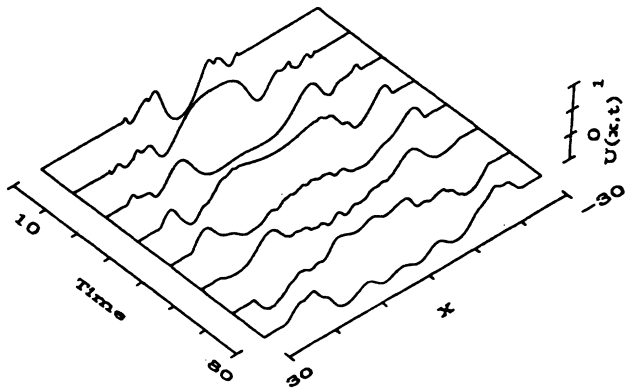

FIG. 8. Creation of radiation, with parameters $T=0.1$, $L=5$, and $A=7$.

$A_1 < A_* < A_2$. In principle, when $T \sim 1$ we could have A_* greater than A_2. If $A_1 < A < A_*$, i.e., $v^2 < v_{\rm cr}^2$, the kink-antikink pairs will annihilate due to the dissipation losses.

In actual experiments LJJ's or EPFM will have a long, yet finite length $L_{\rm tot}$, hence all preceding results will be valid when $L_{\rm tot} \gg \xi_0$. If $L < \xi_0$, which could occur with very low dissipation, the condition for a kink to arrive at the other edge of the system appears as $|h_0| > \exp(-L_{\rm tot})$ and is independent of the initial kink velocity.

IV. NUMERICAL SIMULATION

We have integrated the model equation (9) using the following scheme (see Refs. 23 and 24):

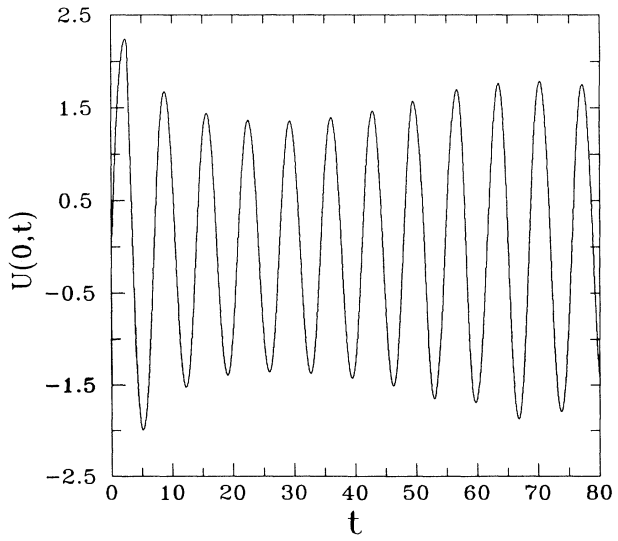

FIG. 9. $u(0,t)$ vs time. The parameters are $T=0.1$, $L=5$, and $A=18$.

$$\frac{u_l^{n+1}-2u_l^n+u_l^{n-1}}{\Delta t^2}-\frac{u_{l+1}^n-2u_l^n+u_{l-1}^n}{\Delta x^2}-\frac{\cos u_l^{n+1}-\cos u_l^{n-1}}{u_l^{n+1}-u_l^{n-1}}+\alpha\frac{u_l^{n+1}-u_l^{n-1}}{2\Delta t}+f_l^n=0\ . \tag{91}$$

For the SG equation without perturbations ($\alpha=0$, $f=0$) there is a discrete energy that is constant:

$$E^n=\tfrac{1}{2}\sum_l \Delta x\left[\frac{u_l^{n+1}-u_l^n}{\Delta t}\right]^2+\tfrac{1}{2}\sum_l \Delta x\left[\frac{u_{l+1}^{n+1}-u_l^{n+1}}{\Delta x}\right]\left[\frac{u_{l+1}^n-u_l^n}{\Delta x}\right]+\sum_l \Delta x\left[1-\frac{\cos u_l^{n+1}+\cos u_l^n}{2}\right]\ . \tag{92}$$

The stability and convergence of the scheme, in this case, have been studied in Ref. 24.

In our numerical simulations, we always take the mesh size $\Delta x=2\Delta t$, with either $\Delta x=0.02$ or 0.04. The spatial integration interval is taken as $(-40,40)$. Two kinds of boundary conditions are used: For the search of kink-antikink thresholds, we simply take $u(-40)=u(40)=0$. For the search of the breather thresholds we add a large damping term γu_t to the left-hand side of Eq. (9) in the spatial intervals $(-40,-35)$ and (35,40) because in this case we have to perform the simulation in a rather long temporal interval; by adding the damping at both ends of the spatial interval, we can avoid reflection effects. Since the theoretical results are obtained in the case $T\ll 1$ (T is the duration of the pulse force), we always take $T=0.1$ in the numerical simulation.

First, we investigate the threshold for generating a kink-antikink pair. In the case of a narrow pulse, we choose two values of L, namely, $L=0.02$ and 0.04, and take $\Delta x=0.02$ and $\Delta x=0.04$, respectively. For $L=0.02$, we found out that the threshold for generating the pair is around $A=3210$, while the theoretical formula gives $A_{\rm thr}^{K\bar{K}}=2\pi/TL+4/\pi L=3205$; for $L=0.04$, the numerical threshold is found to be around $A=1610$, while the theoretical formula predicts that $A_{\rm thr}^{K\bar{K}}=1603$. In the case of wide pulse ($L\gg T$), we also found that the numerical results are in very good agreement with those given by explicit equations (68) and (69). For example, let $L=0.2$. The theory predicts that $A_{\rm thr}$ should be around 332.4, while our numerical simulation shows that $A_{\rm thr}=330$. For $L=10$, the theoretical and numerical $A_{\rm thr}$ are 22.6 and 23.0 respectively. Numerical experiments have been performed for many other values of L ranging from 0.2 to 10.0. The results are presented in Figs. 4–6.

Second, we have investigated the threshold for generating breather, in the case $L=5$. The temporal integration intervals are chosen to be (0,80) and (0,200). The threshold for generating a breather is found to be $14<A<18$, while the theoretical formula gives $A_{\rm thr}^{\rm br}=2\pi/TL\simeq 13$. See Figs. 7–12.

Third, all the above simulations are made with no dissipation in the model (9). If instead we take $\alpha>0$ when $t\le T$, and $\alpha=0$ when $t>T$, all the threshold values will increase, as has been predicted by theoretical analysis.

Finally we point out that the energy input formula [Eq. (83)] is very accurate as checked by the discrete energy [Eq. (92)]. For example, if $T=0.1$, $L=0.02$, and $A=3210$, Eq. (83) gives $E_{\rm input}=206$, while Eq. (92) gives $E=210$ if $T=0.1$, $L=5$, and $A=28$, we have $E_{\rm input}=19.6$, while the numerical energy is $E=19.8$. Obviously, these results also indicate that the case $L\gg T$ is more effective than the case $L\ll T$ for generating solitons.

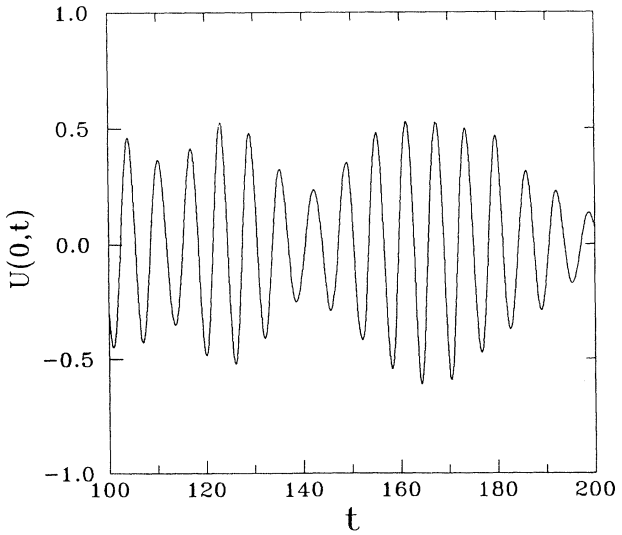

FIG. 10. $u(0,t)$ vs time. The parameters are $T=0.1$, $L=5$, and $A=14$.

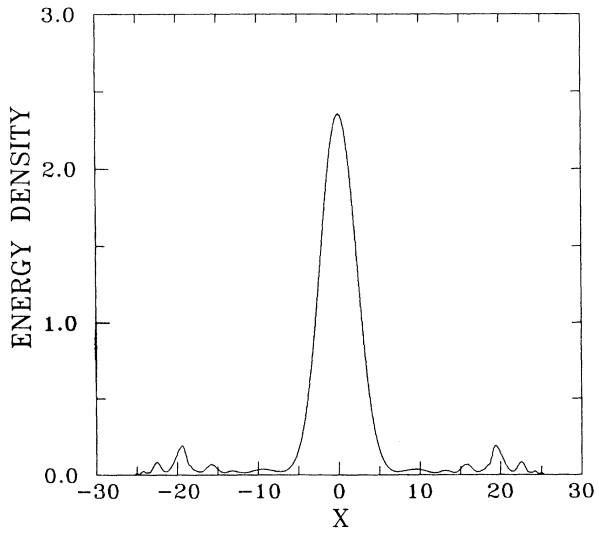

FIG. 11. Energy density at $t=80$. The parameters are $T=0.1$, $L=5$, and $A=18$.

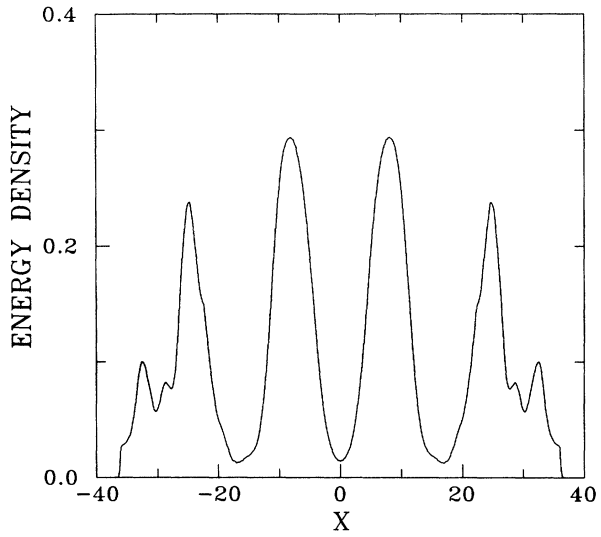

FIG. 12. Energy density at $t=200$. The parameters are $T=0.1$, $L=5$, and $A=14$.

V. CONCLUSIONS

In the preceding sections we have studied the soliton generation problem of SG equation excited by a pulse force with a short duration ($T\sim 0.1$). In two cases, the spatial length L of the pulse force being either larger or smaller than T, the inverse scattering transform method is employed to estimate the thresholds for generating either breather or kink-antikink pairs. The analysis shows that, in order to generate a soliton, the pulse area must exceed a certain threshold value. The thresholds are obtained analytically and checked by numerical simulation. We find that the theoretical and the numerical results are in good agreement.

We notice that the case $L \gg T$ is more effective than the case $L \ll T$ for generation of solitons, because in the latter case ($L \ll T$) most of the input energy is wasted for generating useless radiation, and only a small part of the input energy is contributed to the generation of solitons.

Our results are directly related to physical applications. The problem is applied to the creation of fluxons in long Josephson junctions and magnetic solitons in a one-dimensional magnetic system with an easy-plane anisotropy.

ACKNOWLEDGMENTS

The authors want to thank A. M. Kosevich, V. L. Sobolev, T. K. Soboleva, and A. V. Ustinov for useful discussions. One of the authors (L.V.) thanks North Atlantic Treaty Organization (NATO) for financial support under Grant No. RG674-88. One of us (Z.F.) is grateful to the Liaison Committee of Rectors Conferences of the Member States of the European Communities for financial support. We are indebted to P. Pascual and A. Sánchez for their help in the computations.

[1]A. Barone and G. Paterno, *Physics and Applications of the Josephson Effect* (Wiley, New York, 1982).
[2]A. M. Kosevich, B. A. Ivanov, and A. S. Kovalev, *Nonlinear Magnetization Waves: Dynamical and Topological Solitons* (Naukova Dumka, Kiev, 1983) (in Russian).
[3]S. Sakai, H. Akoh, and H. Hayakawa, J. Appl. Phys. Jpn. Pt.2 **23**, L610 (1984); **24**, L771 (1985).
[4]S. Sakai and M. R. Samuelsen, Appl. Phys. Lett. **50**, 1107 (1987).
[5]N. F. Pedersen, in *Solitons*, edited by S. E. Trullinger, V. L. Pokrovsky, and V. E. Zakharov (North-Holland, Amsterdam, 1986).
[6]D. Hackenbracht and H. G. Schuster, Z. Phys. B **42**, 367 (1981).
[7]I. L. Lyubchansky V. L. Sobolev, and T. K. Soboleva, Fiz. Nizk. Temp. **13**, 1061 (1987) [Sov. J. Low Temp. Phys. **13**, 603 (1987)].
[8]B. A. Kalinikos, N. G. Kovshikov, and A. N. Slavin, Pis'ma Zh. Eksp. Teor. Fiz. **38**, 343 (1983) [JETP Lett. **38**, 413 (1983)].
[9]V. S. Gornakov, L. M. Dedukh, and V. N. Nikitenko, Pis'ma Zh. Eksp. Teor. Fiz. **39**, 199 (1984) [JETP Lett. **39**, 236 (1984)].
[10]P. Degasperis, R. Harcelli, and G. Miceoli, Phys. Rev. Lett. **59**, 481 (1987).
[11]D. J. Kaup, Stud. Appl. Math. **54**, 165 (1975).
[12]V. G. Kamensky, Zh. Eksp. Teor. Fiz. **87**, 1262 (1984) [Sov. Phys. JETP **87**, 723 (1984)].
[13]Yu. S. Kivshar and B. A. Malomed, Zh. Eksp. Teor. Fiz. **95**, 742 (1989) [Sov. Phys. JETP **68**, 421 (1989)].
[14]Yu. S. Kivshar and B. A. Malomed, Fiz. Tverd. Tela **31**, 209 (1989) [Sov. Phys. Solid State **31**, 293 (1989)].
[15]Yu. S. Kivshar and B. A. Malomed, Rev. Mod. Phys. **61**, 763 (1989).
[16]K. J. Mikeska, J. Phys. C **11**, L29 (1978).
[17]S. P. Novikov, S. V. Manakov, L. P. Pitaevisky, and V. E. Zakharov, *Theory of Solitons, The Inverse Scattering Method* (Consultants Bureau, New York, 1984).
[18]V. G. Kamensky and Z. N. Kudriasheva, Physica B+C (Amsterdam) **145B**, 353 (1987).
[19]D. J. Mclaughlin and A. C. Scott, Phys. Rev. A **18**, 1652 (1978).
[20]A. M. Kosevich and Yu. S. Kivshar, Fiz. Nizk. Temp. **8**, 1270 (1982) [Sov. J. Low Temp. Phys. **8**, 644 (1982)].
[21]M. M. Bogdan, A. M. Kosevich, and I. V. Manzhos, Fiz. Nizk. Temp. **11**, 991 (1985) [Sov. J. Low Temp. Phys. **11**, 547 (1985)]; N. Gronbech-Jensen, Yu. S. Kivshar, and M. R. Samuelsen (unpublished).
[22]J. Rubinstein, J. Math. Phys. **11**, 258 (1970).
[23]P. J. Pascual and L. Vazquez, Phys. Rev. B **32**, 8305 (1985).
[24]Guo Ben-Yu, P. J. Pascual, M. J. Rodriguez, and L. Vazquez, Appl. Math. Comp. **18**, 1 (1986).